JOURNAL OF GEOPHYSICAL RESEARCH, VOL. 102, NO. D16, PAGES 19,543–19,557, AUGUST 27, 1997

Local upper tropospheric/lower stratospheric clear-sky water vapor and tropospheric deep convection

Xiaohan Liao[1] and David Rind

Institute for Space Studies, NASA Goddard Space Flight Center, New York

Abstract. Local upper tropospheric and stratospheric water vapor profile retrievals by Stratospheric Aerosol and Gas Experiment II for July 1986–1990 are compared with concurrent International Satellite Cloud Climatology Project deep convective clouds to investigate the possible impact of deep convection on upper level moisture distributions. Results show that at low latitudes, clear-sky water vapor values in the upper troposphere (above 300 mbar level) decrease following the onset of convection, perhaps because of compensatory subsidence. The drying lasts for a few hours and then is interrupted by a moistening trend centered at 6 hours after the convection breaks out, perhaps because of the detrainment of cloud liquid water from the convective tower and spreading anvil clouds. From about 9 hours later the tropical lower stratosphere shows moistening occurring. Largely because of these effects, the tropical lower stratosphere has 20–30% more moisture at sunrise compared to sunset. The later stratospheric moistening has the largest correlation significance with convection as well as the largest sampling number, though the absolute variation is much less than the variation in the troposphere. At northern hemisphere summer middle latitudes, upper tropospheric drying follows moist convection events, without an obvious moistening trend in the upper troposphere and impact in the stratosphere. The results indicate that the relationship between local upper tropospheric moisture and convective events is timescale and latitude dependent. They illustrate the utility of high vertical and temporal resolution data for proper averaging and interpretation of convection and water vapor studies.

1. Introduction

Upper tropospheric water vapor is a crucial factor for maintaining our current climate primarily through its greenhouse absorption. Variations in upper tropospheric water vapor may have significant climatic implications [*Hansen et al.*, 1984; *Kelly et al.*, 1990; *Lindzen*, 1990; *Del Genio et al.*, 1994]. In particular, a smaller absolute change of water vapor at these altitudes can lead to a greenhouse effect equivalent to that of a much larger absolute change in the lower troposphere [*Shine and Sinha*, 1991].

The sources and sinks of upper tropospheric water vapor are still largely unclear. One possible water vapor source is the advection of water vapor from lower levels by tropospheric deep convection. In response to the rising vertical motion in the moist deep convective plume, there may be precipitation due to saturation and condensation and the compensatory subsidence in the vicinity (of the order of a few hundred kilometers). Both the precipitation and the compensatory subsidence would produce drying; on the other hand, the detrained moisture at the top end of the convective towers may increase the atmospheric humidity over wide areas associated with the occurrence and subsequent dissipation of anvil cirrus clouds. The moisture blown out of the wall of convective plumes or reevaporated rainfall may also provide moistening at somewhat lower elevations. These various processes result in the current distribution of upper level moisture, although an exact balance due to convection alone is not guaranteed; the role of large-scale and eddy vertical transports may also be important [*Del Genio et al.*, 1991].

Similar uncertainties concern the stratospheric water vapor budget. Though stratospheric chemical reactions may account for some water vapor, the primary source of stratospheric water vapor is via the upper troposphere. The exact method of entry is largely uncertain: it may be dynamically driven by large-scale upward circulation over tropical regions, by deep convective disturbances close to the tropopause in tropopause folding events, by turbulence associated with jet stream streaks, by gravity-wave-induced turbulence, by evaporation of ice associated with overshooting cirrus clouds, etc.

A primary source of water vapor data for the upper troposphere comes from nadir-looking instruments (e.g., TIROS operational vertical sounder (TOVS) water vapor retrievals). Though the global horizontal coverage of such instruments is good, the vertical resolution is very limited, and the distinction between the upper troposphere and lower stratosphere is often poorly resolved. At the other extreme, radiosonde data have good vertical resolution but poor spatial coverage, with barely one third of the troposphere sampled; the water vapor sensors are also often poorly calibrated.

Despite these data problems, the relationship between upper tropospheric/lower stratospheric moisture and convective events has been the focus of numerous studies, both observational and modeling [*Arakawa and Schubert*, 1974; *Newell and Gould-Stewart*, 1981; *Page*, 1982; *Danielsen*, 1982a; *Hansen et al.*, 1984; *Lindzen*, 1990; *Betts*, 1990; *Rind et al.*, 1991, 1993; *Del Genio et al.*, 1991; *Sun and Lindzen*, 1993; *Soden and Fu*, 1995].

[1]Also at Science Systems and Applications Inc., New York.

Paper number 97JD01258.
0148-0227/97/97JD-01258$09.00

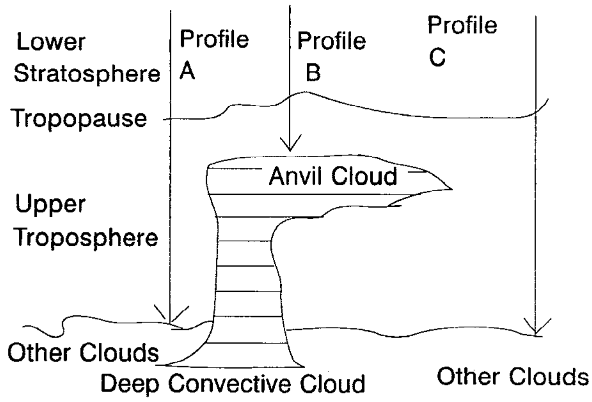

Figure 1. A simple illustration of typical Stratospheric Aerosol and Gas Experiment (SAGE) II measurements of water vapor profiles near local deep convective clouds.

A variety of results have been obtained, with the diversity at least partly associated with the data quality. In addition, the data sets used have had different temporal or spatial scales. For example, some studies have used climatological or monthly average values of convection and water vapor, without necessarily employing matched data. Temporal resolution is also important, considering the short lifetime of convective events (5–10 hours) [*Danielsen*, 1982b].

In this study we explore the relationship between convective events (including the related subsidence) and local upper tropospheric/lower stratospheric water vapor using matched data sets from the Stratospheric Aerosol and Gas Experiment II (SAGE II) [*McCormick et al.*, 1979] and the International Satellite Cloud Climatology Project (ISCCP) [*Rossow et al.*, 1991]. SAGE II retrievals produce clear-sky water vapor profiles with vertical resolution of about 0.5–1 km in the troposphere and 1–2 km in the stratosphere, with a horizontal footprint of about 200 km [*Rind et al.*, 1993; *Chu et al.*, 1993]. Using a limb occultation technique, SAGE II observes the atmosphere at sunrise and sunset only, with typically 30 atmospheric profiles sampled globally per day. Near-global coverage from about 79°N to 79°S can be accumulated after a few weeks, as the satellite orbit plane precesses. The data used in this study are from 1986–1990; after June 1991 the eruption of Pinatubo interrupted water vapor retrievals.

ISCCP cloud observations (stage C1) represent the global, merged results from four to six satellites reporting every 3 hours at a spatial resolution of about 280 km (often converted into a 2.5° × 2.5° resolution for practical use, as in this study) [*Rossow et al.*, 1991]. One cloud type produced as a data product from ISCCP is that of "deep convective clouds," clouds with (large) optical thickness greater than 23 and cloud top pressure less than 440 mbar. The deep convective clouds require visible channel optical thickness, so they are unavailable at night. The deep convective cloud fraction, calculated as the percent of convective pixels on a 30 km scale among the total pixels, is a good quantity to denote the overall deep convective activity.

A simple illustration of the spatial relationship between SAGE II and ISCCP measurements is given in Figure 1. SAGE II clear-sky retrievals may be occurring above the ISCCP deep convective clouds (profile B); they may be occurring within the clear sky associated with compensatory subsidence (profile A); or they may be retrieving water vapor in a portion of the grid unrelated to the convective activity (profile C). Whatever the situation, which is likely to vary from case to case, the results do not include the moisture contained within the anvil cloud, and therefore total moisture, clear plus cloudy skies, cannot be obtained. In the lower stratosphere this situation does not arise; the presence of clouds in the lower stratosphere over low latitudes affects less than 1% of the SAGE II data.

2. Method

A SAGE II water vapor profile retrieval covers an atmospheric column with a latitudinal horizontal footprint of about 200 km at one particular time at the sampling rate of, typically, every 50 minutes. For ISCCP deep convective clouds the horizontal coverage is near global but daytime only, with reporting every 3 hours at a spatial resolution of about 280 km. For accurate comparison between water vapor and deep convection it is important that each individual SAGE II water vapor profile is matched with an ISCCP convection observation. As described in detail by *Liao et al.* [1995a, b], SAGE II site information (latitude and longitude) is converted into the corresponding ISCCP grid box, and the SAGE II sampling time is rounded up to every 3 hours (starting from 0000 UT) to match ISCCP. Therefore the time error for SAGE II after the change is ±1.5 hours (as is the case for ISCCP). Any hour value cited in this study therefore has an error of up to ±1.5 hours.

To investigate both the instant and the gradual response of the atmospheric water vapor content to deep convection events, each SAGE II water vapor profile is matched with the deep convection observations (frequencies) taken concurrently at the same location and at times 3, 6, 9, 12, 15, 18, and 21 hours earlier (if available). Statistically, this is equivalent to taking each convective event and then comparing the water vapor profiles at 3 hour intervals afterward; the first approach is used because the ISCCP data has more temporal flexibility than the SAGE II observations, which are only for sunrise and sunset. Though, in theory, each SAGE II retrieval may have eight sequential ISCCP measurements from time differences 0–21 hours, the absence of ISCCP deep convection data at night can greatly limit the available number of matched observational pairs. For instance, if a SAGE II observation occurs at sunrise, there will be no matched ISCCP convective data for 3 or 6 hours earlier as the relevant site is still in darkness (polar regions are not included here). A summary chart is shown in Figure 2 depicting the availability of SAGE–ISCCP matched pairs and the associated event types (sunrise/sunset) of SAGE II data. For matched SAGE-ISCCP observations, if the ISCCP sampling time is between 0 and 6 hours earlier than SAGE II, only SAGE II sunset data are available. If the ISCCP sampling time is between 15 and 21 hours earlier than SAGE II, only SAGE II sunrise data are available. The only time that SAGE II may have both sunrise and sunset observations matched with ISCCP is for 9 to 12 hours earlier than SAGE II. The number of available matches ranges between 800 and over 1700, typically about half sunrise and half sunset events. Because the shorter daytime over southern middle latitudes in July does not provide sufficient daytime convective data to match the water vapor for a complete time span of 0–21 hours, we do not include southern hemisphere middle latitudes in this study. The focus on summer results minimizes the consideration of the role of extra tropic eddies.

The histogram of the number of available ISCCP-SAGE II matched observations versus ISCCP convective fractions is shown in Figure 3. The number of available pairs is greatly reduced at high convective fractions; this is consistent with the relevant infrequent occurrence of deep convection occupying the totality of a 62,500 km^2 area.

To eliminate the strong impact associated with geographical (particularly latitudinal) dependence of water vapor, all water vapor values used throughout this study are in the form of a relative percentage of the local climatological mixing ratio unless otherwise stated. For example, a water vapor amount of 110% would indicate that the water vapor mixing ratio is 10% greater than its local climatology, as determined from all available data for that locality (pressure level and grid box).

The water vapor profiles originally are for each kilometer altitudinal level from the upper stratosphere down to cloud tops or to the tropospheric boundary layer if the atmosphere is sufficiently transparent. At a fixed altitude level, water vapor variations may occur simply because of the daily fluctuation in the height of the pressure level associated with the daily cycle of atmospheric temperature. To minimize this effect, all water vapor profiles were interpolated to nine pressure levels: 500, 300, 200, 150, 100, 70, 50, 30, and 10 mbar. Pressure levels greater than 500 mbar are not studied here because of the insufficient number of samples, and pressure levels less than 10 mbar are not discussed either since they may contain potentially large retrieval errors [*Rind et al.*, 1993].

The temperature and tropopause data used here are those which are included in the SAGE II data set. They are not measured by SAGE II itself but are provided by the National Meteorological Center (NMC) (now known as the National Centers for Environmental Prediction) for each SAGE II retrieval time and location and therefore is applicable to the water vapor and cloud data used in this study.

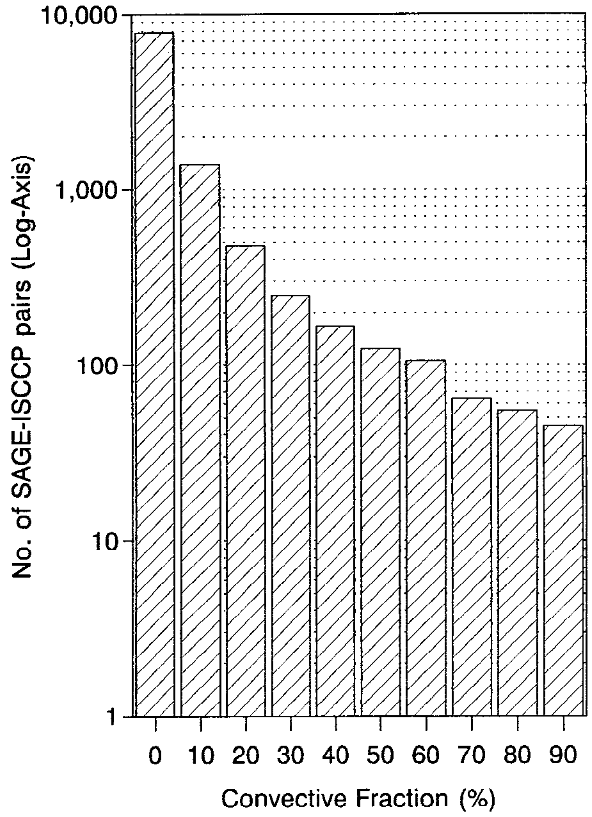

Figure 3. Histogram of the number of available ISCCP-SAGE matched observations versus ISCCP convective fractions for July 1986–1990.

3. Results

3.1. General Trends

Using the matched data sets described in the previous section, the general relationship between convection and water vapor profiles at various hours after the detection of the convection event is presented in Figure 4. Results for low latitudes (30°S–30°N) are presented in Figures 4a–4c, and results for northern hemisphere summer middle latitudes (30°N–60°N) are presented in Figures 4d–4f. Figures 4a and 4d show results when there is essentially no convection within the ISCCP grid (less than 10% of the pixels show deep convection); these serve to show that there is no data bias associated with the convection-free situation. Figures 4b and 4e are for moderate deep convection (10–50% of the pixels); Figures 4c and 4f are for enhanced deep convection (greater than 50%). As described before, the water vapor value given is as a percent of its local climatology.

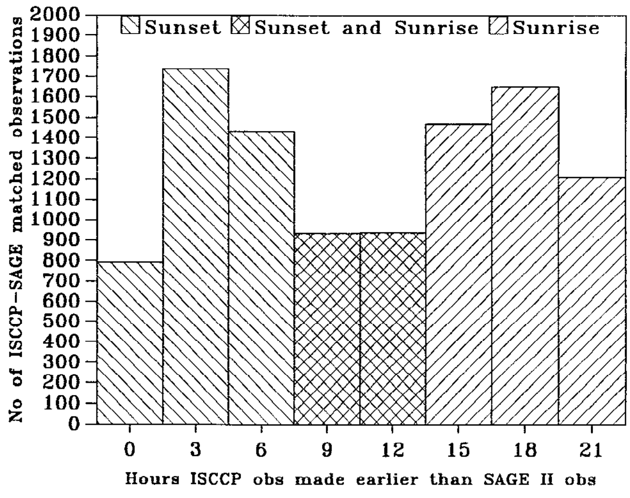

Figure 2. Number of available International Satellite Cloud Climatology Project (ISCCP)-SAGE matched observations and the availability of SAGE II sunrise or sunset data when ISCCP-SAGE sampling time difference is from 0 to 21 hours for July 1986–1990.

Figure 5 corresponds to Figure 4, except that it illustrates the penetration rate of SAGE II samplings under different convection-free and convection-affected situations to indicate the relative amount of available retrievals used in Figure 4. Areas with less than five samplings are shown in Figure 4 and Figure 5 as having no data. As indicated earlier, a particular hour cited can have an error range up to ±1.5 hours.

The results in Figure 4 indicate that in both latitude ranges when there is no convection (<10%), there is no water vapor change (<10%) in our selected data set either contemporaneously or afterward (Figures 4a and 4d). Though other factors like large-scale condensation clouds could affect the water vapor, they may not be captured by SAGE II measurements because of the obscuring effect of cloud cover. With moderate convection (10–50%) at low latitudes, there is initially drying aloft from 300 to 150 mbar for the first three hours (Figure 4b). The effect then fades away to be replaced by moistening from 6–12 hours after detection of convection. (In this study, "after convection" implies after the initial detection of convection

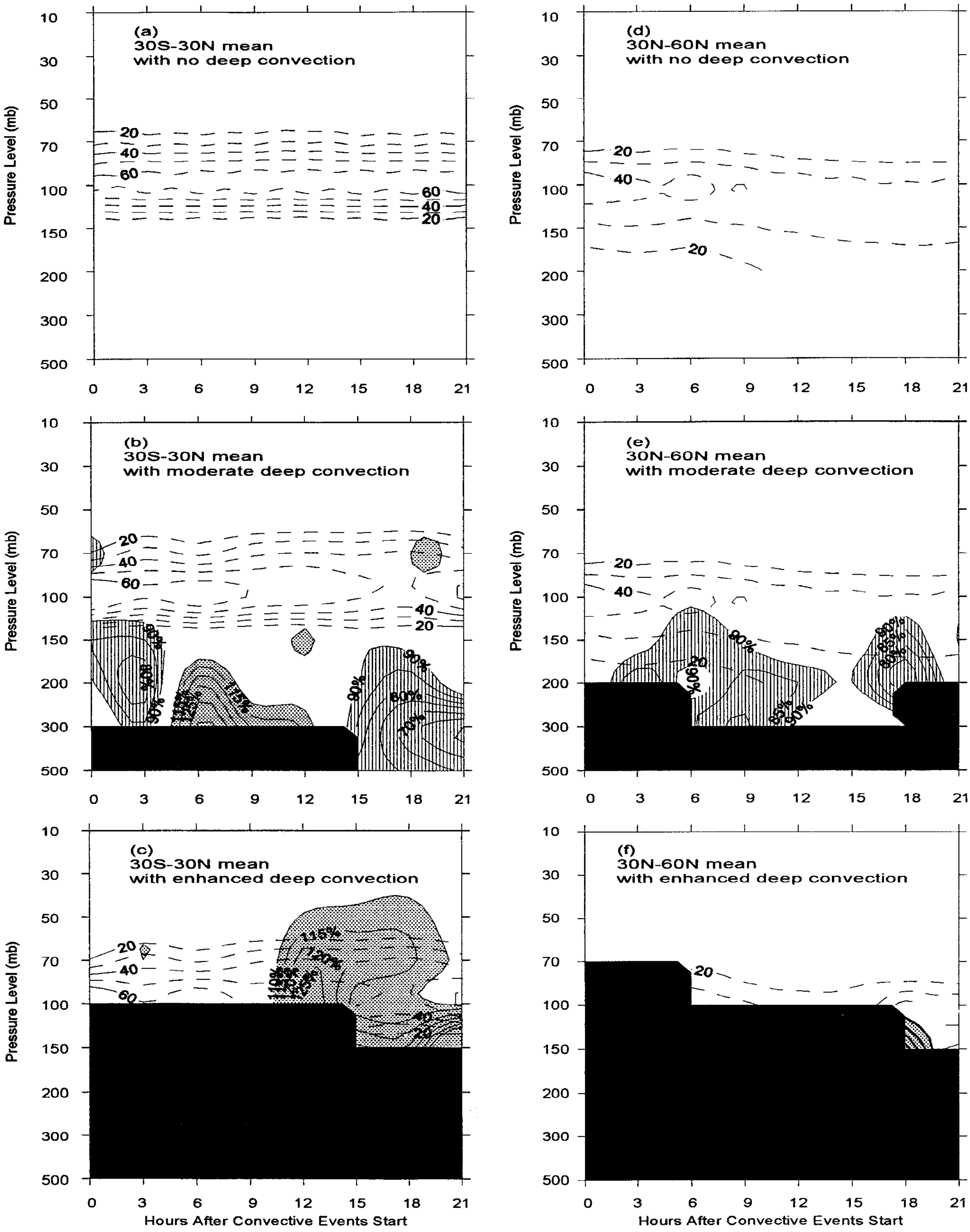

Figure 4. SAGE II mean water vapor change (percent of its local climatology) versus time (hour) after ISCCP detection of (a) and (d) no deep convection, (b) and (e) moderate deep convection, or (c) and (f) enhanced deep convection for July 1986–1990. Solid contour lines are for water vapor variation. Solid contour lines with vertical line-shading are for water vapor less than 90%, and the dotted-shading for more than 110%. Dashed contour lines are for the distribution percentage of tropopause pressure. Areas with solid areas denote insufficient sampling (less than five samples).

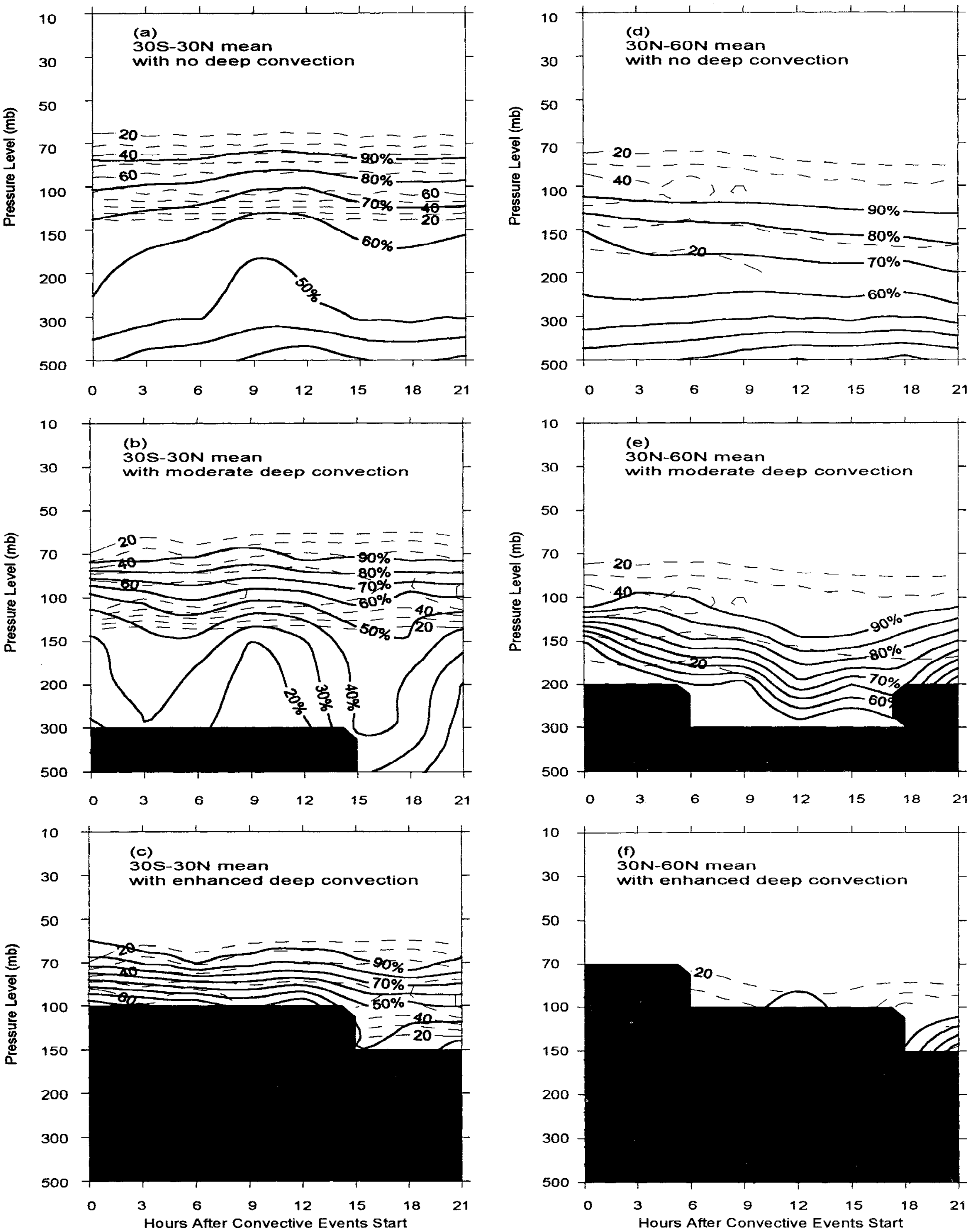

Figure 5. As in Figure 4 but for the SAGE II penetration probability (percent) (solid lines).

rather than after the end of convection). From 15–21 hours, drying is once again apparent. With enhanced deep convection (>50%) the reduced penetration rate of SAGE II prevents sufficient sampling for the tropical upper troposphere; however, a significant area of moistening above 100 mbar is seen beginning 9–12 hours afterward and extending through the end of the period (Figure 4f). The moistening maximum is centered at 12 hours and gradually diminishes in altitude.

Table 1. Frequency Distribution of Tropopause Pressure at Different Delayed Times After Detection of Different Convective Situations for July 1986–1990

	Pressure, mbar	Delayed Times 0 hours	3 hours	6 hours	9 hours	12 hours	15 hours	18 hours	21 hours
				30°S–30°N					
No convective clouds	70–100	27	25	25	26	28	24	24	24
	100–150	67	70	71	72	71	72	72	72
	150–200	3	3	2	1	0	2	3	2
	200–300	0	0	0	0	0	0	0	0
10–50% convective clouds	70–100	21	35	28	38	41	39	42	35
	100–150	75	61	69	59	58	51	47	62
	150–200	0	0	2	2	0	9	7	2
	200–300	0	0	0	0	0	0	2	0
>50% convective clouds	70–100	31	45	47	27	33	35	38	22
	100–150	68	55	52	72	66	65	61	77
	150–200	0	0	0	0	0	0	0	0
	200–300	0	0	0	0	0	0	0	0
				30°N–60°N					
No convective clouds	70–100	12	11	14	11	7	7	7	5
	100–150	49	42	45	40	36	33	31	34
	150–200	26	29	25	29	31	33	33	33
	200–300	12	15	14	18	23	23	25	24
10–50% convective clouds	70–100	6	11	16	8	2	10	0	0
	100–150	43	34	40	32	28	26	44	38
	150–200	31	34	32	32	28	24	13	19
	200–300	18	19	12	23	40	36	37	42
>50% convective clouds	70–100	0	20	12	10	0	0	0	0
	100–150	50	40	50	20	71	14	30	50
	150–200	50	20	25	40	0	28	20	33
	200–300	0	20	12	30	28	57	50	16

Frequency distributions are given as percents. The time error is ±1.5 hours.

At midlatitudes the results are somewhat different. For moderate convection the drying which is seen initially is basically maintained throughout the day. Even with enhanced convection, while no data for the troposphere is available (because of heavy cloudy coverage), the data for the lower stratosphere show no moistening trend.

Table 1 gives the frequency distribution of the tropopause pressure at different times after detection of different convective situations, and Figure 6 further displays the smoothed contour maps of vertical distribution for selected cases. For 30°S–30°N the tropopause pressure is mostly between 70 and 150 mbar, suggesting that the drying and moistening associated with the moderate convection (Figure 4b) is mostly below the tropopause while the moistening with enhanced convection (Figure 4c) is largely visible in the tropopause region and lower stratosphere. For 30°N–60°N the tropopause pressure variations are much larger than for 30°S–30°N, and the drying with the modest convection at the middle latitudes occurs frequently at the tropopause region.

3.2. Significance and Magnitudes of the Drying and Moistening Trends

The results shown in Figure 4 are the mean tendencies following convective events discretized into gross categories. Because SAGE II cannot see through clouds, the number of available SAGE II observations is limited by the presence of convective and other optically thin clouds; the climatological average is biased toward clear sky, making the statistics less reliable in the troposphere than in the lower stratosphere.

To evaluate the significance of the correlation between water vapor amount and the convective fraction, correlation coefficients are shown in Figure 7 along with their significance levels. The lower stratospheric moistening seen in Figure 4 6 hours after convective initiation appears to occur in the middle and upper troposphere as well (Figure 4b), but because of the reduced samplings, its significance is lower. According to the correlation and significance charts, the largest correlation (up to 0.5) and the most significant area (>99%) occur near the tropical tropopause and in the lower stratosphere where the moistening trend appears. An example of the good relationship in terms of climatological average between convective fraction and lower stratospheric moistening at low latitudes is shown in Figure 8, which displays the 70 mbar water vapor amount at various delayed times versus the amount of deep convective fraction detected. The tropospheric significance levels for both 30°S–30°N and 30°N–60°N are less than the tropical lower stratosphere due at least partly to the reduced number of data available and the much larger variation in the tropospheric water vapor.

To estimate the magnitude of the variations implied in Figure 4, Figure 9 presents the climatological profile of absolute water vapor amount (ppmv) versus pressure at low latitudes. The water vapor reaches its minimum value between 100 and 70 mbar, which is just above the averaged tropopause height (110 mbar). Above the height associated with the lowest water vapor amount (the hygropause) the lower stratospheric water vapor increases with decreasing atmospheric pressure. Comparison between Figures 4 and 9 indicates that the drying and moistening occurs in the regions where the absolute water vapor amount is relatively low and the signature of relative changes is easier to detect. Since water vapor mean changes in Figure 4 are in the form of a relative percentage of climatology, comparison with Figure 9 shows that the drying and moistening

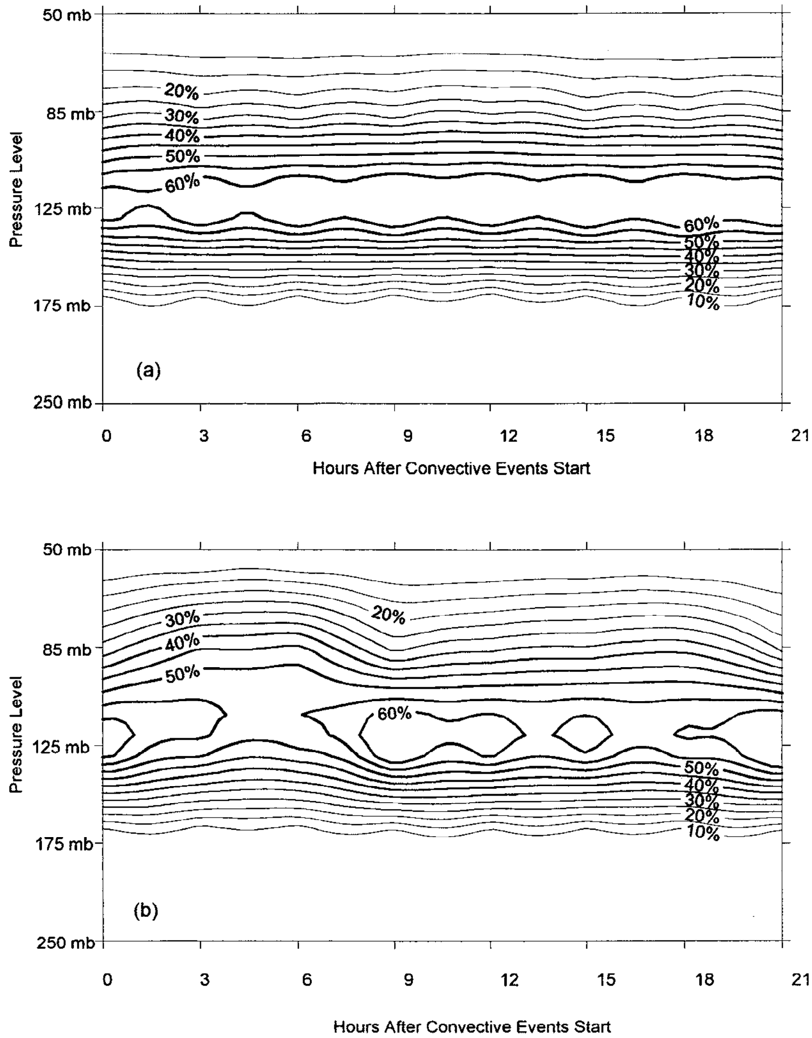

Figure 6. Vertical frequency distribution (percent) of tropopause versus pressure at different delayed time after detection of cases with (top) convection-free and (bottom) enhanced convection at 30°S–30°N. July 1986–1990.

in the upper troposphere can be easily greater than 20–30 ppmv at 300 mbar and 5–10 ppmv at 200 mbar. The moistening in the lower stratosphere is generally around 1 ppmv.

3.3. Implications of Upper Tropospheric Trends

The optical thickness for convective clouds can be easily a few hundred times larger than the maximum optical thickness that SAGE II can see through. Therefore the variation of the water vapor inside any cloud body that happens to be present is basically unknown. Furthermore, it is also not known where the clear sky observed by SAGE II is relative to the convective plume (Figure 1). In part, the low correlation significance in some regions may be due to the mixture of locations. Therefore any interpretation of the results shown in Figures 4 and 6 must of necessity involve considerable speculation; nevertheless, the data do suggest a plausible physical interpretation.

Compensatory subsidence should be associated with the convective plume. Analysis of the deep convective cloud tops indicates that the cloud top pressure is mostly 150–220 mbar. The upper tropospheric drying for the first 3 hours is between the 300 and 150 mbar level, therefore at and below the cloud top altitude, and would be consistent with subsidence-induced drying as the downward motion advects air from higher and drier altitudes. This does not indicate that the total moisture at these levels is reduced since the cloud moisture is unobservable.

After 3 hours the drying disappears, and from 6–12 hours a moistening occurs. The moistening is centered at the 300 mbar level and extends to 200 mbar, substantially below the tropopause indicated in Table 1. The period of 6–12 hours after the detection of convection is roughly consistent with the typical lifetime of 5–10 hours for tropospheric convective events [*Danielsen*, 1982b; *Pfister et al.*, 1993; W. B. Rossow, personal communication, 1996]. Therefore, by this time it is likely that a significant portion of the convection-related clouds has dissipated, with detrainment and evaporation of the cloud liquid water adding to the clear-sky background moisture. In addition, the dispersion of convective-related clouds allows SAGE II to see through some ex-cloudy atmosphere to regions where water vapor, which has been advected from below in the convective plume, resides. By this time also the clear atmosphere has been gradually affected by the moisture blown out of the convective plumes since the beginning of the convective event.

By 15 hours after the convective event, another drying trend occurs. An explanation for this effect can be derived from

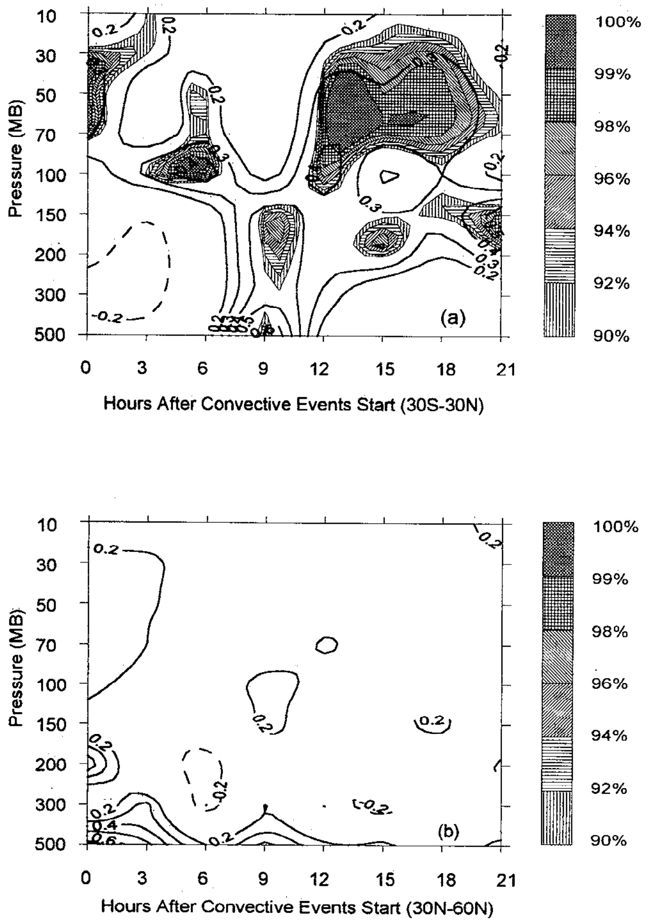

Figure 7. Correlation coefficients and their significance levels between water vapor change and convective fraction for (top) 30°S–30°N and (bottom) 30°N–60°N. The solid contour lines indicate the correlation coefficients, and the pattern-shading contours indicate the significance level. July 1986–1990.

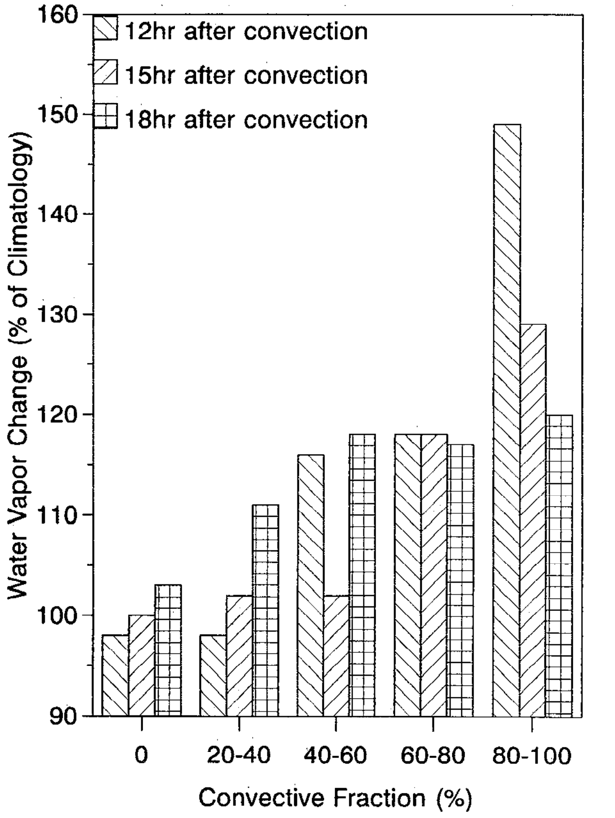

Figure 8. The 70 mbar mean water vapor change (as a percent of local water vapor climatology) 12–18 hours after ISCCP detection of different fractions of deep convection clouds for 30°S–30°N, July 1986–1990.

Figure 5b. At 9–12 hours, there is a secondary minimum in penetration rate, which is therefore a secondary maximum in convective clouds. Water vapor retrievals sampled at 9 hours or later are substantially associated with sunrise events (Figure 3). There is ample observational evidence in support of a large diurnal cycle of convection over this region, with the maximum occurrence in later afternoon [*Nitta and Sekine*, 1994] and a secondary maximum near sunrise [*Gary and Jacobson*, 1977; *Hendon and Woodberry*, 1993]. Therefore, at 9–12 hours the moistening which begins at 6 hours is interrupted by the contemporaneous convective drying, a tendency which eventually overpowers the clear-sky moistening trend in the locality, and finally prevails from 15–21 hours when the impact of the convection detected 15–21 hours ago becomes of second-order importance.

This last result may be relevant for interpreting the midlatitude observations. As shown in Figure 4e, no moistening is evident following convection. Either the convective drying associated with each event has more/longer influence at middle latitudes or the convective events themselves may be more continuous. Extratropical summer convection can occur either in isolation, as air mass thunderstorms, or in (front-related) clusters. The occurrence of clusters increases the effective duration of convection; at midlatitudes, SAGE II may be effectively seeing the results of convection extending through the "moistening" period evident at low latitudes. Although we do not have nighttime data to provide a full analysis, on the basis of ISCCP daytime observations, we can calculate the autocorrelation of deep convective clouds to estimate their duration in

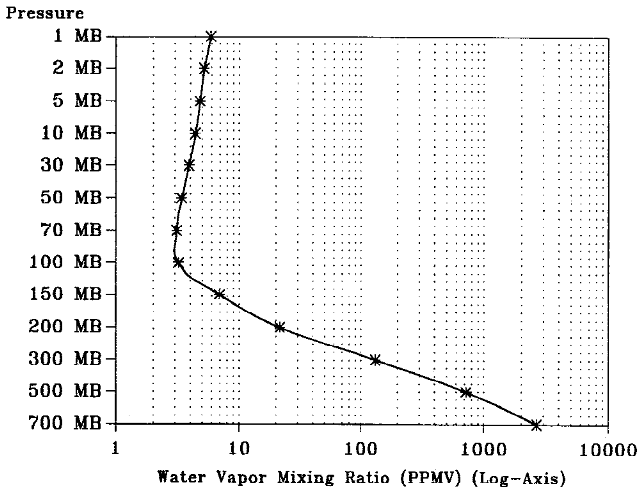

Figure 9. Absolute water vapor amount (ppmv) versus pressure levels for 30°S–30°N. July 1986–1990. The height associated with the minimum water vapor (hygropause) normally is around 2 km above the tropopause.

the different latitude bands. The results are shown in Table 2: convective events do happen more continuously at midlatitudes than at low latitudes, especially for the 6–9 hour period after initial detection, the time when tropical tropospheric moistening is maximum. Similarly, Table 3 indicates the 200 mbar SAGE II penetration rate versus time after detection of deep convection; it shows a greater penetration rate at low latitudes at the time of maximum moistening (6 hours after detection) again implying less persistent convection at low latitudes. Note that while this may be one explanation for the differences seen in Figure 4, it does not rule out the possibility that there may be other differences between tropical and extratropical convection.

3.4. Implication of the Moistening Trend in the Tropopause Region and the Lower Stratosphere

The cloud impact is close to zero in the tropopause region and lower stratosphere at low latitudes. This means that in contrast to the situation in the upper troposphere, the moisture changes seen at these levels are the total moisture, and there is no sampling bias toward clear-sky conditions. Therefore the mean moistening trend in the tropopause region and the lower stratosphere shown in Figure 4c can be used to indicate a net increase in water vapor content. Part of the variation in the vertical extent of the moistening largely reflects the vertical variations of the tropopause pressure as shown in Table 1. But the topmost moistening at and above the 70 mbar height indicates variation in the lower stratosphere.

The impact of convective events on the stratosphere-troposphere exchange may include the convective erosion of the tropopause [*Price and Vaughan*, 1993], gravity-wave-induced small-scale turbulence, or radiative heating of anvils [*Russell et al.*, 1993]. The physical mechanism by which convection relates to the tropopause and lower stratospheric moistening cannot be conclusively investigated with the data available here. On the basis of the results, however, one possible explanation is that with enhanced convective events, for the first 6 hours the tropopause is pushed upward as characterized by the lower tropopause pressure for the first 6 hours, compared with the nonconvective or moderate convective situation (Table 1 and Figure 6). Then, 9–12 hours later, when most of the convective events end and the radiative cooling has had some time to function, the tropopause descends (indicated by the increase in tropopause pressure). At this time some of the upper tropospheric water vapor provided by the convection may enter into the low stratosphere.

The reason why water vapor enters into the lower stratosphere significantly at low latitudes with no significant changes at northern middle latitudes (Figures 4 and 7, bottom right) is not completely clear. However, even at low latitudes, moderate convection (Figure 4b) does not apparently moisten the lower stratosphere, so perhaps midlatitude events are not sufficiently penetrative. Furthermore, since the upper troposphere is not being moistened (Figure 4e), there is less likelihood that the lower stratosphere will be. Again, the upper troposphere difference may be the result of more frequent convection, as discussed previously, or it may imply a real difference in the convective process.

Table 2. Autocorrelation Coefficient Between Convective Events Versus Lagged Time for July 1986–1990

	Lagged Hours							
Region	0	3	6	9	12	15	18	21
30°S–30°N	1.00	0.62	0.41	0.26	0.47	N/A	N/A	N/A
30°N–60°N	1.00	0.56	0.50	0.40	0.35	N/A	N/A	N/A

The time error is ±1.5 hours. The values are significant at the 99% level.

Table 3. SAGE II Penetration Rate at 200 mbar Versus Time After Detection of Deep Convection for July 1986–1990

	Hours After the Convective Events							
Region	0	3	6	9	12	15	18	21
30°S–30°N	44	41	70	41	66	64	73	62
30°N–60°N	46	57	55	52	74	65	70	50

Penetration rates are given as percents. The time error is ±1.5 hours.

3.5. Sunrise and Sunset: Water Vapor Global Distributions Versus Convection

As noted in section 2, the study of instant and delayed responses in water vapor content to deep convection perturbations was made in such a way as to maximize the use of the frequent temporal coverage of ISCCP cloud data. Another way to explore the relationship with convection is to see if there is any significant difference between sunrise and sunset water vapor climatologies. Figure 10 shows the water vapor distribution at the pressure levels of 70 (near the tropopause in the tropics) and 100 mbar (mostly tropopause regions) for sunrise and sunset. The water vapor values are larger at sunrise between about 30°S and 30°N. The magnitude of the difference is 0.5–1 ppmv (typically 20–30% of the background values); as the increase occurs throughout most of this region, which occupies 50% of the area of the globe, it is therefore globally significant. Similar differences between sunrise and sunset are also obvious for 50 mbar (not shown). According to the previous analysis, lower stratospheric water vapor change may be positively correlated with deep convection activities that happened about a dozen hours ago. As shown in Figure 2, SAGE II water vapor has sunrise and sunset data available if the ISCCP-SAGE II time difference is 9–12 hours, and this provides us a chance to examine whether the deep convection 9 or 12 hours prior to sunrise is significantly different from that before sunset.

Indeed, consistent with the above analysis, calculation of global and regional mean convective amounts indicate greater convective fractions 9–15 hours before sunrise than 9–15 hours before sunset (Table 4). Shown in Figure 11 is the global distribution of convection 9–12 hours before sunrise and sunset. Though there are regions of enhanced convective activities at sunrise, enhanced convection 9–12 hours before sunrise overwhelmingly occurs in the major convective regions (Figure 11, bottom): the extreme western equatorial Pacific, the North Atlantic storm track area, central America, and the African monsoon region. Apparently, tropospheric moisture enters the stratosphere from locations such as these preferentially at sunrise because of the diurnal variation of convection and the lag time for transference into the stratosphere. In some locations, convection maximizes 9–12 hours before sunset, for example, in the vicinity of Indonesia one of the few locations in which

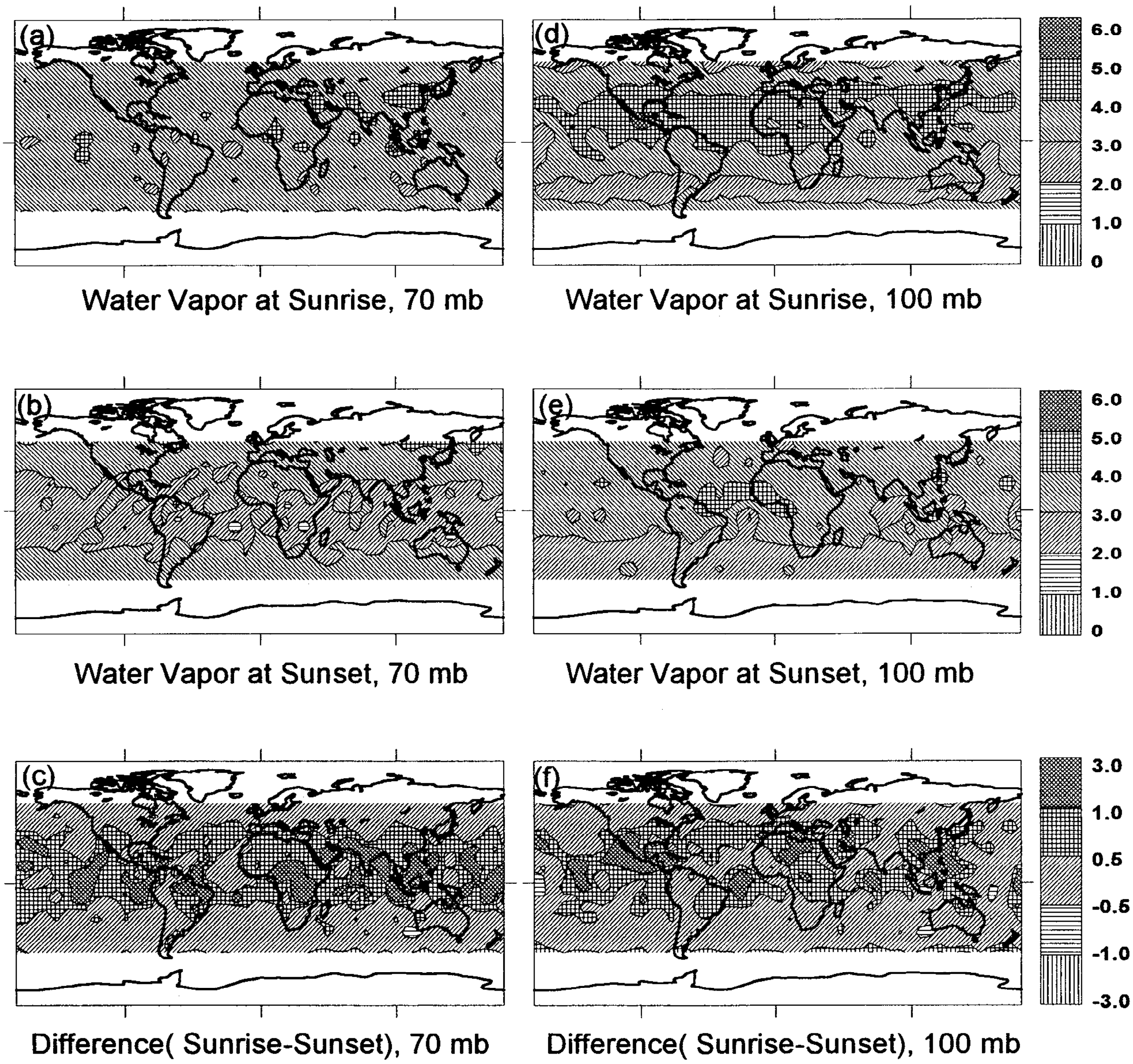

Figure 10. Monthly mean global distribution of water vapor mixing ratio (ppmv) at (left) 70 mbar and (right) 100 mbar for (top) sunrise and (middle) sunset events and the (bottom) difference (sunrise-sunset) distribution for July 1986–1990.

the 100 mbar water vapor is actually larger at sunset (Figure 10).

3.6. Analysis of Retrieval Uncertainties

Both the SAGE II water vapor and the ISCCP convective data used in this study have some uncertainties that can potentially contaminate the results discussed in the previous sections. In addition, there are other diurnal variations which could affect the interpretation of the results shown in Figure 10. In this section we discuss some of these uncertainties.

As shown in Figure 3, the results for 0–6 hours in Figure 4 are contributed by sunset measurements only and those of 15–21 hours are contributed by sunrise measurements. This suggests that the results in Figure 4 may be influenced by diurnal changes of water vapor content. However, Figures 4a and 4d show that without convective events, there is no diurnal variation (greater than 10%).

The most natural reason for the sunrise and sunset difference in the lower stratosphere is the daily fluctuation of levels associated with diurnal temperature variations. For this study, by comparing data in pressure coordinates (rather than in

Table 4. Global Mean Deep Convection Fraction at Different Hours Before Local Sunrise and Sunset Events for July 1986–1990

	Hours Before the Sunrise/Sunset Events							
Event	0	3	6	9	12	15	18	21
Sunrise	6.5	N/A	N/A	6.7	8.2	6.1	5.2	4.7
Sunset	6.4	5.4	5.4	5.5	6.6	1.5	N/A	N/A

Convection fractions are given as percents. The time error is ±1.5 hours.

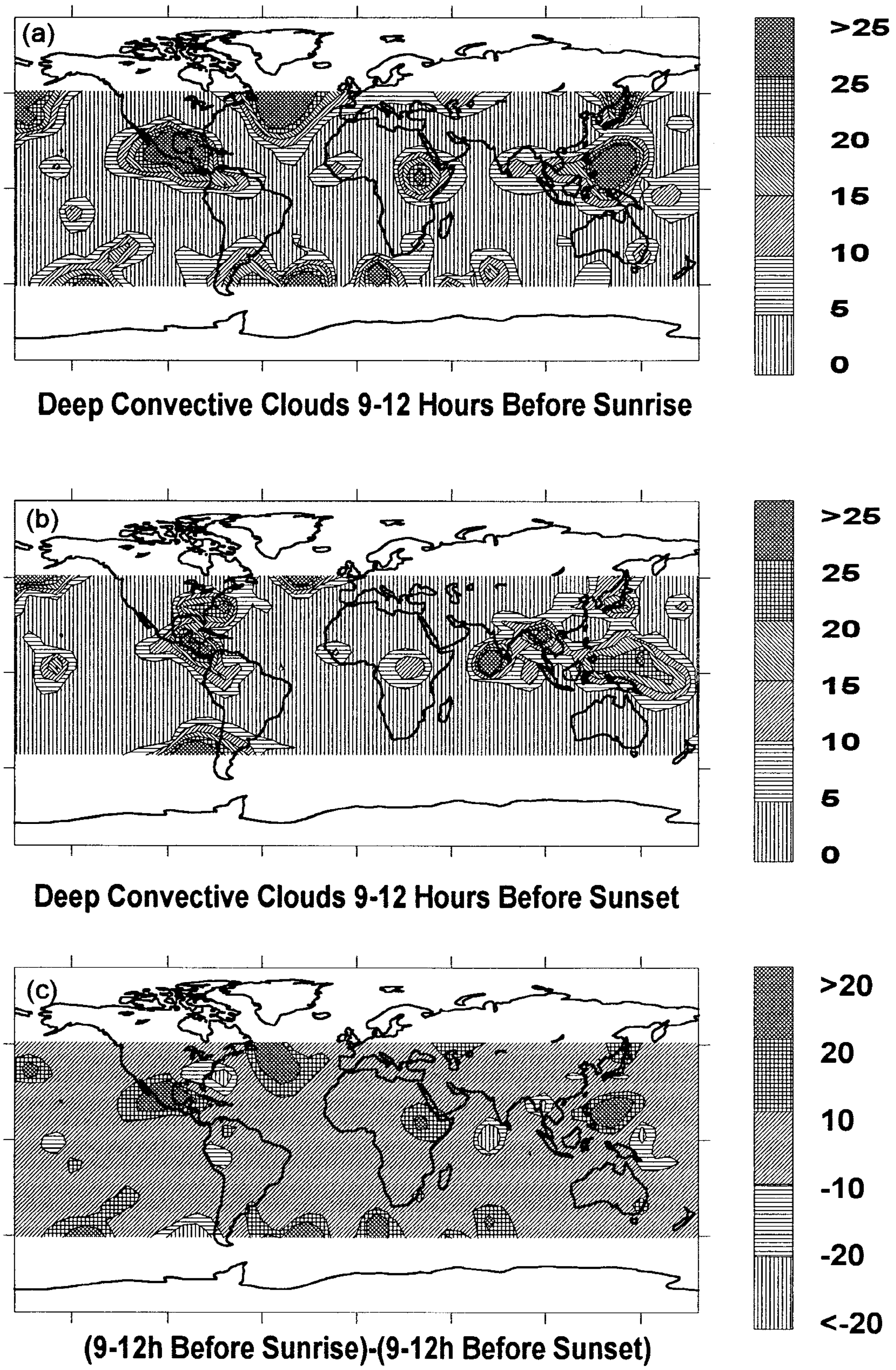

Figure 11. Monthly mean global distribution of convective factions (percent) occurring (top) 9–12 hours before sunrise, (middle) 9–12 hours before sunset, and (bottom) the difference for July 1986–1990.

altitude) this potential problem has been eliminated. However, diurnal variations in temperature could still affect the results by altering the saturation vapor pressure at the tropopause.

Figure 12 shows the atmospheric temperature for sunrise and sunset at the 70 and 100 mbar levels. There is little diurnal temperature change in the tropopause or the lower stratosphere at low latitudes; the biggest difference occurs over northern middle latitudes (as seen in Figure 12, bottom).

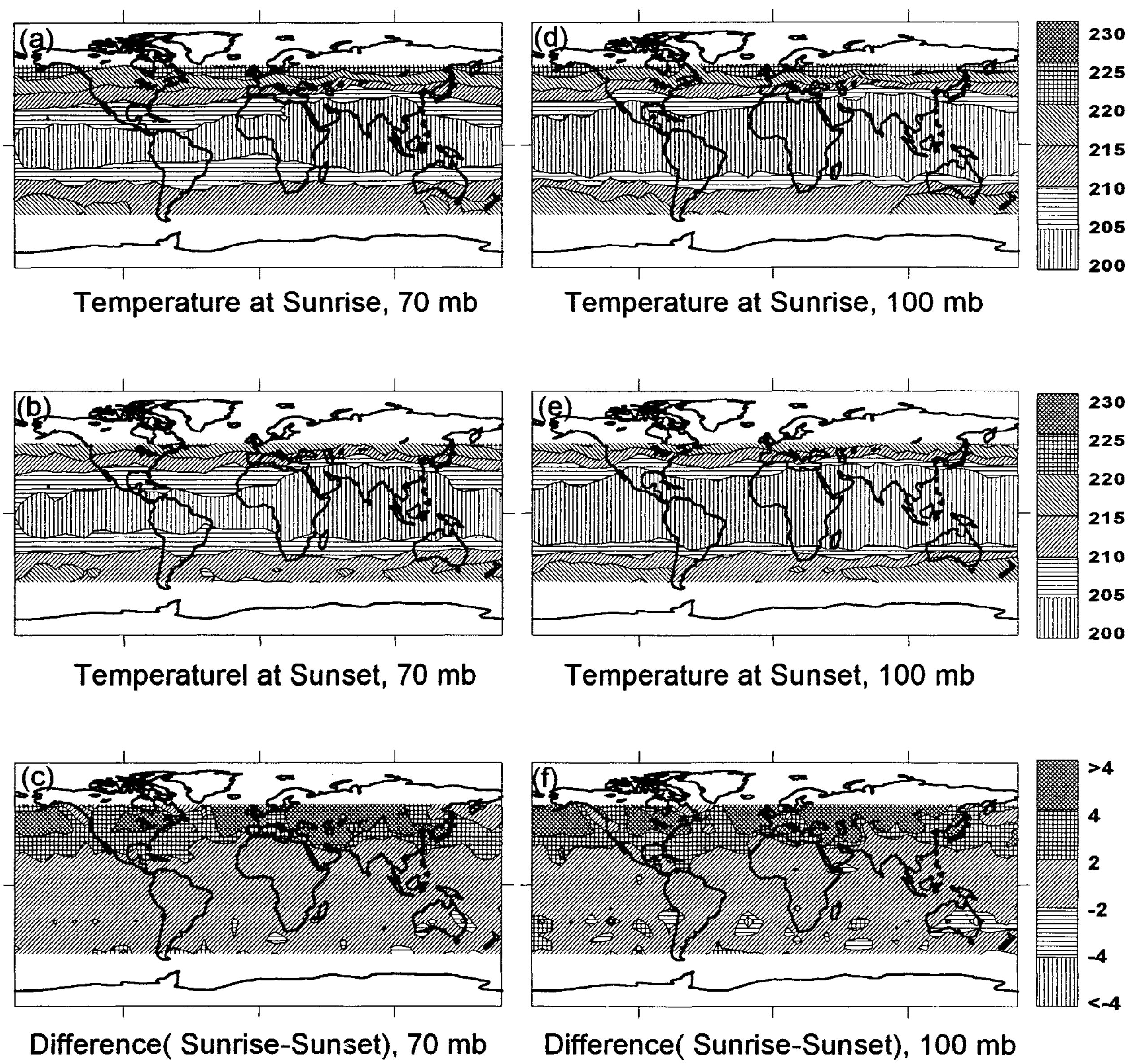

Figure 12. The same as Figure 10 but for atmospheric temperature (kelvins).

Therefore we cannot relate the sunrise-sunset water vapor difference to a diurnal temperature fluctuation. No correlation between the water vapor diurnal cycle and the temperature diurnal cycle was found to be significant.

The water vapor retrievals depend upon removal of the aerosol component. While the data retrieval process attempts to remove aerosols, there is some uncertainty as to the accuracy of this process. Therefore a diurnal variation of aerosol could possibly contaminate the water vapor retrieval.

Shown in Figure 13 is the SAGE II aerosol extinction at 1.02 μm at 70 and 100 mbar for sunrise and sunset. At 100 mbar the aerosol extinction values at low latitudes are mostly greater than 0.0008 per kilometer, indicating substantial presence of high-level clouds at this level. While difference do arise, there is no consistent relationship between the aerosol and water vapor tendencies. (*Rind et al.* [1993] noted that when aerosols impact SAGE water vapor retrievals, they usually result in increased water vapor values.) At 70 mbar, while there is scattered increase in aerosol concentration at sunrise, the tropical water vapor increase is much more widespread and not particularly colocated with the aerosol change. The aerosol differences are also quite small and should not affect the water vapor retrievals. It is interesting to note that if the delayed water vapor increase in the lower stratosphere is associated with the troposphere-stratosphere (mass) exchange as suggested before, one might expect a similar increase for aerosols in the lower stratosphere, as the air mass that carries the moisture into the stratosphere should also transport the upper tropospheric aerosols which were advected from lower elevation by the convection events. This effect is not particularly evident in Figure 13; it could be minimized because of the factors, including rainout, associated with convection.

A noticeable increase in sunset aerosol extinction occurs over northern high latitudes. Although this effect is occurring in summer, it is similar in phase to the diurnal cycle of polar stratospheric clouds (PSCs) in winter, which also appear more often at sunset in the SAGE II data. In both seasons, diurnal variations in vertical motion could account for the results;

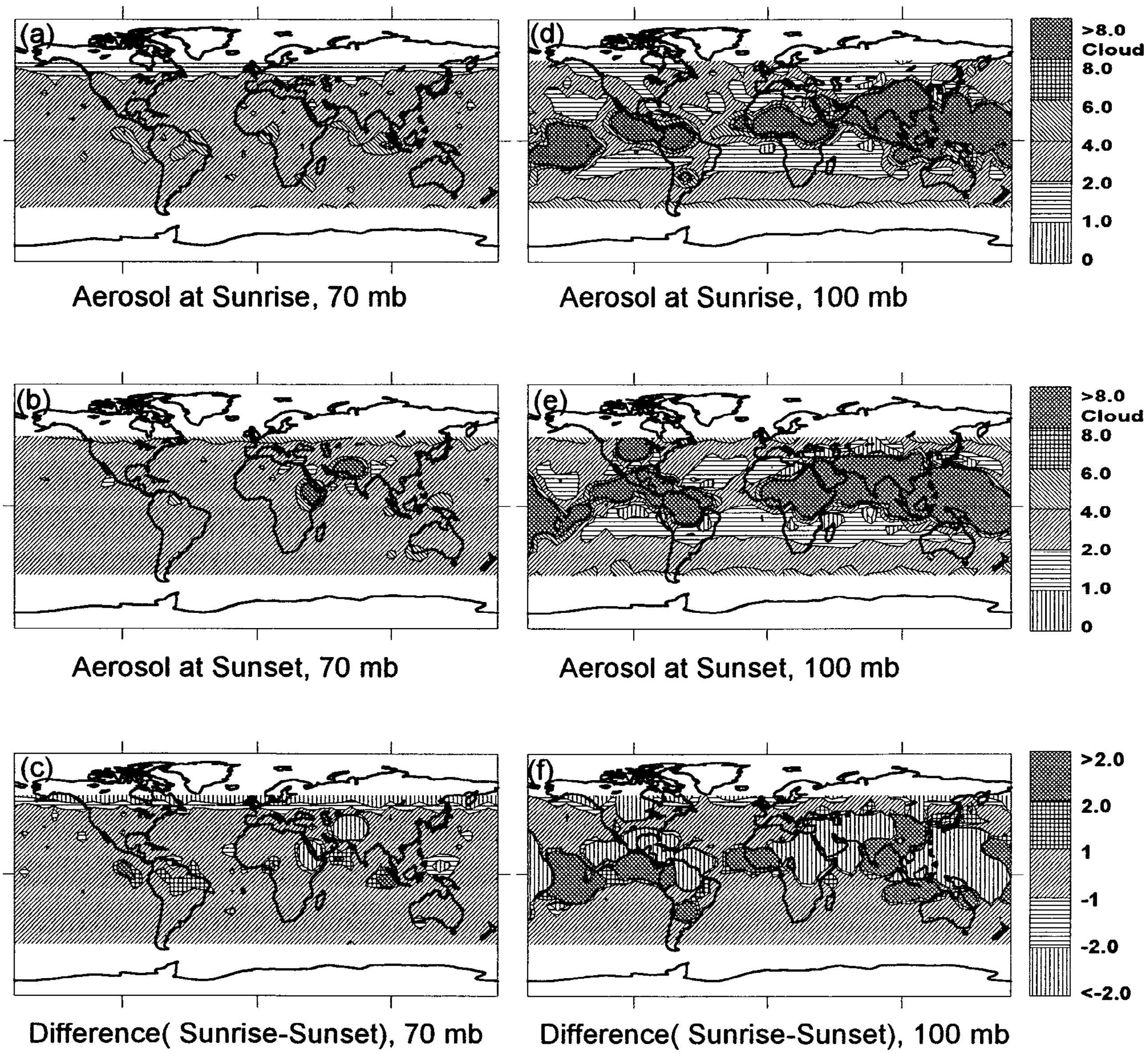

Figure 13. The same as Figure 10 but for aerosol extinction coefficient at 1.02 μm wavelength (10^{-4} km^{-1}). Aerosol extinction values greater than 8 (10^{-4} km^{-1}) are regarded as substantially affected by high-level clouds.

when increased upward vertical motion occurs at these latitudes during sunset (a time of generally reduced stability in the troposphere), it would increase the lower stratospheric aerosol concentration and also provide for colder temperatures, leading to more PSCs. As can be seen in Figure 13, colder temperatures do occur at sunset during July at these latitudes.

For ISCCP deep convection the deep convection clouds were identified using only two thresholds: cloud top pressure and cloud optical thickness. The classification has been shown to be good at low latitudes, but the clear distinction between deep convective clouds and other thick clouds may be less reliable in the middle latitudes, with larger uncertainties [*Rossow and Garder*, 1993]. Therefore, from the perspective of ISCCP deep convective data, results for low latitudes have the highest reliability.

4. Summary and Discussion

The following are the primary results of this study:

1. In the tropical upper troposphere (300–150 mbar), for the first few hours after moderate deep convection is detected, clear-sky water vapor decreases by some 20% compared to local climatology, amounting to changes of about 20–30 ppmv at 300 mbar and 5–10 ppmv at 200 mbar. This is interpreted as the effect of compensatory subsidence, drying the clear air. This effect then fades away, and from 6 to 12 hours after detection a moistening is observed of the same order of magnitude as the previous drying. This is interpreted as indicating the effect of detrained cloud moisture, now largely present in the clear sky, given the average convective lifetime of 5–10 hours. Drying again occurs in the tropical upper troposphere 12–15 hours after initial detection; this may be interpreted as the result of subsidence drying in the upper troposphere air associated with secondary maximum occurrence of convection. At middle latitudes in northern hemisphere summer, upper tropospheric drying appears to follow convective events throughout the day. A partial interpretation of this difference from low latitudes results from the observation that the mid-

latitude convection lasts longer than tropical convection, overlapping the moistening period.

2. A moistening trend is observed in the tropical tropopause regions and lower stratosphere beginning at 9–12 hours after the detection of enhanced convection in the troposphere; the percentagewise effect is similar to that observed at lower levels, and in terms of magnitude it amounts to about 1 ppmv. This is interpreted as an input of upper tropospheric moisture provided by deep convection into the lower stratosphere due to factors possibly including variation in the tropopause pressure. Daily fluctuation in the tropical lower stratospheric water vapor mixing ratio is also found with water vapor values about 20–30% higher during sunrise than during sunset; this is explained as the result of the diurnal variation of enhanced deep convection, which maximizes 9–12 hours before sunrise, and the lag time for water vapor getting into the tropical stratosphere is 9–12 hours. No significant variation is found in the tropopause region and the lower stratosphere at middle latitudes, possibly because of the lack of upper tropospheric moistening associated with the convection.

The effect of convection on the local moisture distribution in the upper troposphere is a subject of debate. If convection had no net effect and convection was the only important process, then there would be no time or space variations in upper tropospheric moisture. Clearly, this is not the case. *Rind et al.* [1991] noted that on climatological and seasonal timescales, when in-cloud effects have presumably been fully resolved, the upper troposphere has more moisture in seasons and locations with increased convection. Similar results are reported by *Inamdar and Ramanathan* [1993] and *Soden and Fu* [1995]. This is in contrast to suggestions that more and deeper convection may lead to the drying of the upper troposphere because of the subsidence on the local cumulonimbus scale [*Lindzen*, 1990]. Either of these conclusions would imply that other processes (e.g., large-scale circulation and/or eddy transports) are important and that convective events have a nonzero net effect locally.

The results here for the 200 km scale suggest that both moistening and drying may occur in the clear air, depending on different latitudes and different timescales; on the immediate timescale (a few hours), clear-sky drying does arise, presumably because of subsidence, but on a longer timescale (6–12 hours), when in-cloud moisture has been detrained, moistening results in the tropics.

In some of the recent work [*Sun and Lindzen*, 1993] the focus was on the large-scale circulation (e.g., tropical convection, subtropical subsidence), so that the net effect globally might be different from that which occurs locally. This paper, focusing on local scales, cannot comment on that issue; circulations on such broad scales, while to some degree forced by convection, involve the large-scale circulation and its budget rather than simply convection per se [e.g., *Rind and Rossow*, 1984].

For the tropopause region and stratosphere, previous results are also somewhat contradictory. *Page* [1982] showed that increased lower stratospheric water vapor is associated with enhanced convective plumes. *Kuhn* [1982] also reported that overshooting convective towers add to the lower stratospheric moistening based on aircraft experiment data. However, some other studies have attributed the dryness of the lower stratosphere to increased convection, either through the effect on the tropopause temperature [*Newell and Gould-Stewart*, 1981] or through a "freeze-drying" procedure associated with convective overshooting [*Danielsen*, 1982a] or with large-scale upwelling in tropical cyclones [*Danielsen*, 1993]. *Kritz et al.* [1993] showed evidence of an effective dehydration process in the lower stratosphere following troposphere-to-stratosphere transport of tropospheric air associated with convective activity. The results here indicate that convection may or may not lead to moistening or drying at the tropopause and in the lower stratosphere, depending on latitudes and observational time.

A major question raised by these results concerns the extent to which the moistening occurs in the tropical lower stratosphere (Figures 4 and 7, bottom left). The moistening impact extends some 20–40 mbar above the tropopause active range (Figure 6) in a period of 18 hours. How the apparent moistening is transmitted over this altitude range in such a short period of time is very uncertain. To produce this effect by a vertical motion alone would require vertical velocities of the order of $2–5 \times 10^{-4}$ mbar s^{-1}; this is an order of magnitude larger than the mean values estimated for the region [e.g., *Peixoto and Oort*, 1992]. It would be hard to ascribe the effect to convective motions since the convection does not show deep penetration into the stratosphere. Deep convection can generate vertically propagating gravity waves. There has been some observational evidence showing that the gravity waves may contribute to the local water vapor profile variations in the stratosphere [*Teitelbaum et al.*, 1994], though in this study the water vapor changes occur well after the gravity waves should have propagated away from the region. As indicated in section 3.6, there is no apparent problem with the data retrieval, which, in any event, would be less likely in these regions of well-sampled stratosphere. The results imply greater vertical mixing in the tropical lower stratosphere than might therefore have been assumed.

This work is based on the combined use of SAGE II water vapor and ISCCP deep convective data. It must be emphasized again that the results obtained here do not all have equal degrees of reliability. As SAGE II water vapor data for the upper and middle troposphere have smaller sampling than for the tropopause and lower stratosphere and the climatology is biased toward the clear-sky because of cloud shielding, the results are more tentative for the upper troposphere than for the lower stratosphere. However, SAGE II continues to function; with the addition of more data we should be able to increase the sampling to better test the tropospheric correlations and to provide an assessment of winter conditions. A better assessment is also needed of the identification of deep convection particularly at middle latitudes. The results so far emphasize the utility of data with high vertical resolution and the necessity of studying convection and water vapor processes with fine temporal resolution and different regions in matched data sets.

Acknowledgments. This work was supported by the SAGE III Science Team and Patrick McCormick, project scientist. W. B. Rossow kindly provided access to the ISCCP cloud data sets. Er-Woon Chiou provided updated SAGE II water vapor data. Tony Del Genio and James Hansen offered helpful comments on earlier versions of the manuscript. Rick Healy helped in graphics programming support.

References

Arakawa, A., and W. H. Schubert, Interaction of a cumulus cloud ensemble with the scale environment, I, *J. Atmos. Sci.*, *31*, 674–701, 1974.

Betts, A. K., Greenhouse warming and tropospheric water vapor budget, *Bull. Am. Meteorol. Soc.*, *71*, 1465–1467, 1990.
Chu, W. P., E. W. Chiou, J. C. Larsen, L. W. Thomson, D. Rind, J. J. Buglia, S. Oltmans, M. P. McCormick, and L. M. McMaster, Algorithms and sensitivity analyses for Stratospheric Aerosol and Gas Experiment II water vapor retrieval, *J. Geophys. Res.*, *98*, 4857–4866, 1993.
Danielsen, E. F., A dehydration mechanism for the stratosphere, *Geophys. Res. Lett.*, *9*, 605–608, 1982a.
Danielsen, E. F., Statistics of cold cumulonimbus anvils based on enhanced infrared photographs, *Geophys. Res. Lett.*, *9*, 601–604, 1982b.
Danielsen, E. F., In situ evidence of rapid, vertical, irreversible transport of lower tropospheric air into the lower tropical stratosphere by convective cloud turrets and by large-scale upwelling in tropical cyclones, *J. Geophys. Res.*, *98*, 8665–8681, 1993.
Del Genio, A. D., A. A. Lacis, and R. A. Ruedy, Simulations of the effect of a warmer climate on atmospheric humidity, *Nature*, *351*, 382–385, 1991.
Del Genio, A. D., W. Kovari, and M.-S. Yao, Climatic implications of the seasonal variation of upper tropospheric water vapor, *Geophys. Res. Lett.*, *21*, 2701–2704, 1994.
Gary, W. M., and R. W. Jacobson Jr., Diurnal variation of deep cumulus convection, *Mon. Weather Rev.*, *105*, 1171–1188, 1977.
Hansen, J., A. Lacis, D. Rind, G. Russell, P. Stone, I. Fung, R. Ruedy, and J. Learner, Climate sensitivity: Analysis of feedback mechanisms, in *Climate Processes and Climate Sensitivity*, *Geophys. Monger. Ser.*, vol. 29, edited by J. E. Hansen and T. Takahashi, pp. 130–163, AGU, Washington, D. C., 1984.
Hendon, H. H., and K. Woodberry, The diurnal cycle of tropical convection, *J. Geophys. Res.*, *98*, 16,623–16,637, 1993.
Inamdar, A. K., and V. Ramanathan, Greenhouse effect over the tropical oceans, relative importance of water vapor and lapse rate variations, in *IRS'92, Current Problems in Atmospheric Radiation*, edited by S. Keenvallik and O. Kaner, pp. 155–157, Deepak, Hampton, Va., 1993.
Kelly, K. K., A. F. Tuck, L. E. Heidt, M. Lowenstein, J. R. Podolske, S. E. Strahan, and J. F. Vedder, A comparison of ER-2 measurements of stratospheric water vapor between the 1987 Antarctica and 1989 Arctic airborne missions, *Geophys. Res. Lett.*, *17*, 465–468, 1990.
Kritz, M. A., S. W. Rosner, K. K. Kelly, M. Loewenstein, and R. K. Chan, Radon measurements in the lower tropical stratosphere: Evidence for rapid vertical transport and dehydration of tropospheric air, *J. Geophys. Res.*, *98*, 8725–8736, 1993.
Kuhn, P. M., Broadland airborne water vapor radiometry, *Geophys. Res. Lett.*, *9*, 621–624, 1982.
Liao, X., W. B. Rossow, and D. Rind, Comparison between SAGE and ISCCP high-level cloud, I, Global and zonal mean cloud amounts, *J. Geophys. Res.*, *100*, 1121–1135, 1995a.
Liao, X., W. B. Rossow, and D. Rind, Comparison between SAGE and ISCCP high-level cloud, II, Locating cloud tops, *J. Geophys. Res.*, *100*, 1137–1147, 1995b.
Lindzen, R. S., Some coolness concerning global warming, *Bull. Am. Meteorol. Soc.*, *71*, 288–299, 1990.
McCormick, M. P., P. Hamill, T. J. Pejin, W. P. Chu, T. J. Swissler, and L. R. McMaster, Satellite studies and stratospheric aerosol, *Bull. Am. Meteorolol. Soc.*, *60*, 1038–1045, 1979.
Newell, R. E., and S. Gould-Stewart, A stratospheric fountain? *J. Atmos. Sci.*, *38*, 2789–2796, 1981.
Nitta, T., and S. Sekine, Diurnal variation of convective activity over the tropical western Pacific, *J. Meteorol. Soc. Jpn.*, *72*, 627–641, 1994.
Page, W. A., NASA experiment on tropospheric-stratospheric water vapor transport in the intertropical convergence zone, *Geophys. Res. Lett.*, *9*, 599–624, 1982.
Peixoto, J. P., and A. H. Oort, *Physics of Climate*, 520 pp., Am. Inst. of Phys., New York, 1992.
Pfister, L., S. Scott, M. Loewenstein, S. Bowen, and M. Legg, Mesoscale disturbances in the tropical stratosphere excited by convection: Observations and effects on the stratospheric momentum budget, *J. Atmos. Sci.*, *50*, 1058–1075, 1993.
Price, J. D., and G. Vaughan, The potential for stratosphere-troposphere exchange in cutoff-low systems, *Q. J. R. Meteorol. Soc.*, *119*, 343–365, 1993.
Rind, D., and W. Rossow, The effects of physical processes on the Hadley circulation, *J. Atmos. Sci.*, *41*, 479–507, 1984.
Rind, D., E.-W. Chu, J. Larsen, S. Oltmans, J. Learner, M. P. McCormick, and L. McMaster, Positive water vapor feedback in climate models confirmed by satellite data, *Nature*, *349*, 500–503, 1991.
Rind, D., E.-W. Chiou, W. Chu, S. Oltmans, J. Lerner, J. Larsen, M. P. McCormick, and L. McMaster, Overview of Stratospheric Aerosol and Gas Experiment II water vapor observations: Method, validation, and data characteristics, *J. Geophys. Res.*, *98*, 4835–4856, 1993.
Rossow, W. B., and L. G. Garder, Validation of ISCCP cloud detections, *J. Clim.*, *6*, 2341–2369, 1993.
Rossow, W. B., L. G. Garder, P. Lu, and A. W. Walker, International Satellite Cloud Climatology Project (ISCCP): Documentation of cloud data, *Tech. Rep. WMO/TD-266* (revised), 76 pp, plus three appendices, World Meteorol. Org., Geneva, 1991.
Russell, P. B., L. Pfister, and H. B. Selkirk, The Tropical Experiment of Stratosphere-Troposphere Exchange Project (STEP): Science objectives, operations, and summary findings, *J. Geophys. Res.*, *98*, 8563–8589, 1993.
Shine, K. P., and A. Sinha, Sensitivity of the Earth's climate to height dependent changes in water vapor mixing ratio, *Nature*, *354*, 382–284, 1991.
Soden, J., and R. Fu, A satellite analysis of deep convection, upper-tropospheric humidity, and the greenhouse effect, *J. Clim.*, *8*, 2333–2351, 1995.
Sun, D.-Z., and R. S. Lindzen, Distribution of tropical tropospheric water vapor, *J. Atmos. Sci.*, *50*, 1643–1660, 1993.
Teitelbaum, H., J. Ovarlez, H. Kelder, and F. Lott, Some observations of gravity-wave-induced structure in ozone and water vapor during EASOE, *Geophys. Res. Lett.*, *21*, 1483–1486, 1994.

X. Liao and D. Rind, Institute for Space Studies, NASA Goddard Space Flight Center, 2880 Broadway, New York, NY 10025. (e-mail: CDXXL@thebes.giss.nasa.gov)

(Received October 29, 1996; revised April 28, 1997;
accepted April 28, 1997.)